

Prospecting for *In Situ* Resources on the Moon and Mars using Wheel-Based Sensors

M. G. Buehler, R. C. Anderson and S. Seshadri

Jet Propulsion Laboratory, California Institute of Technology, 4800 Oak Grove Drive, Pasadena, CA 91109
and

M. G. Schaap, University of California, Riverside

Abstract^{1,2}— The Apollo and Russian missions during 1970's were reviewed to rediscover the type and distribution of minerals on the Moon. This study revealed that the Moon is a relatively barren place in mineral content when compared with the Earth. Results from the Lunar minerals brought back to Earth, indicate that the Moon lacks water, hydroxyl ions, and carbon based minerals. Our approach to prospecting utilizes a vehicle with sensors embedded in a wheel that allow measurements while the vehicle is in motion. Once a change in soil composition is detected, decision making software stops the vehicle and analytical instruments perform a more definitive analysis of the soil. The focus of this paper is to describe the instrumentation and data from the wheel-based sensors.

measurements are influenced by temperature, mineral type, grain size, porosity, and soil conductivity. Nevertheless we propose the use of the following wheel-based sensors:

- Impedance Spectrometer for dielectric permittivity measurements,
- Electrical Conductivity measurements,
- Electrometer for characterizing electrostatic properties using signature analysis techniques, and
- Magnetometer for characterizing magnetic properties.

All of these measurements are rapid and the sensors are small and so can be incorporated into the wheel of a roving vehicle allowing rapid *in situ* measurements.

TABLE OF CONTENTS

INTRODUCTION	1
LUNAR MATERIALS	1
WHEEL-BASED SENSORS	3
IMPEDANCE SPECTROMETER	3
1.1 Lunar Soils and Terrestrial Minerals	4
1.2 Imaginary Permittivity.....	4
ELECTRICAL RESISTIVITY	5
1.3 Moisture detection	5
1.4 Permafrost.....	5
ELECTROMETER	6
1.5 Electrometer	6
1.6 Ottawa Sand.....	6
1.7 Basalt	6
1.8 Titanium Dioxide.....	7
1.9 Hematite	7
MAGNETOMETER	7
CONCLUSION	8
ACKNOWLEDGMENTS	8
REFERENCES	8
BIOGRAPHIES	9

LUNAR MATERIALS

In this study we analyzed the Lunar regolith in order to determine the most dominant minerals. Our results indicate that the Lunar regolith is composed mainly of silicates and oxides. Representatives from these groups are listed in Table. 1. As seen in the table, the elemental composition is also quite restricted for the minerals made up of only ten elements.

Table 1. Lunar Silicates and Oxides

Silicates (Most Abundant)	
Pyroxene	(Ca,Fe,Mg)2Si2O6
Plagioclase feldspar	(Ca,Na)(Al,Si)4O8
Olivine	(Mg,Fe)2SiO4
Potassium feldspar	KAlSi3O8
Silica	SiO2
Oxides (Next in Abundance)	
Ilmenite	FeTiO3
Chromite	FeCr2O6
Ulvospinel	FeTiO4
Hercynite	FeAl2O4
Spinel	MgAl2O4

INTRODUCTION

The approach to prospecting is to identify and locate ISR (In Situ Resources). Thus, our prospecting approach emphasizes looking for minerals on the Lunar surface that employ rapid surveying techniques. Identifying minerals is difficult because of the many parameters that influence the measurements. In particular, soil electrical property

Satellite surveys from Clementine and Lunar Prospector [1] indicate the presence of water especially at the poles of the Moon. These observations indicate that other minerals such as hydroxyls and water should also be included in the likely lunar minerals. But these orbital observations have not been confirmed by *in situ* measurements and so we'll limit our view of the lunar soil to the silicates and oxides. The minerals from the LSB [2] are shown in Fig. 1 and 2 from 14 Apollo and Luna sites. In Fig. 1, the basalts are

¹ 0-7803-8155-6/04/\$17.00 © 2004 IEEE

² Paper Number: 1573/rev1

composed mostly of silicates such as the olivines, feldspars, and pyroxenes. The oxides are shown at the top

of the chart. For the most part, they are less than 20% of the total.

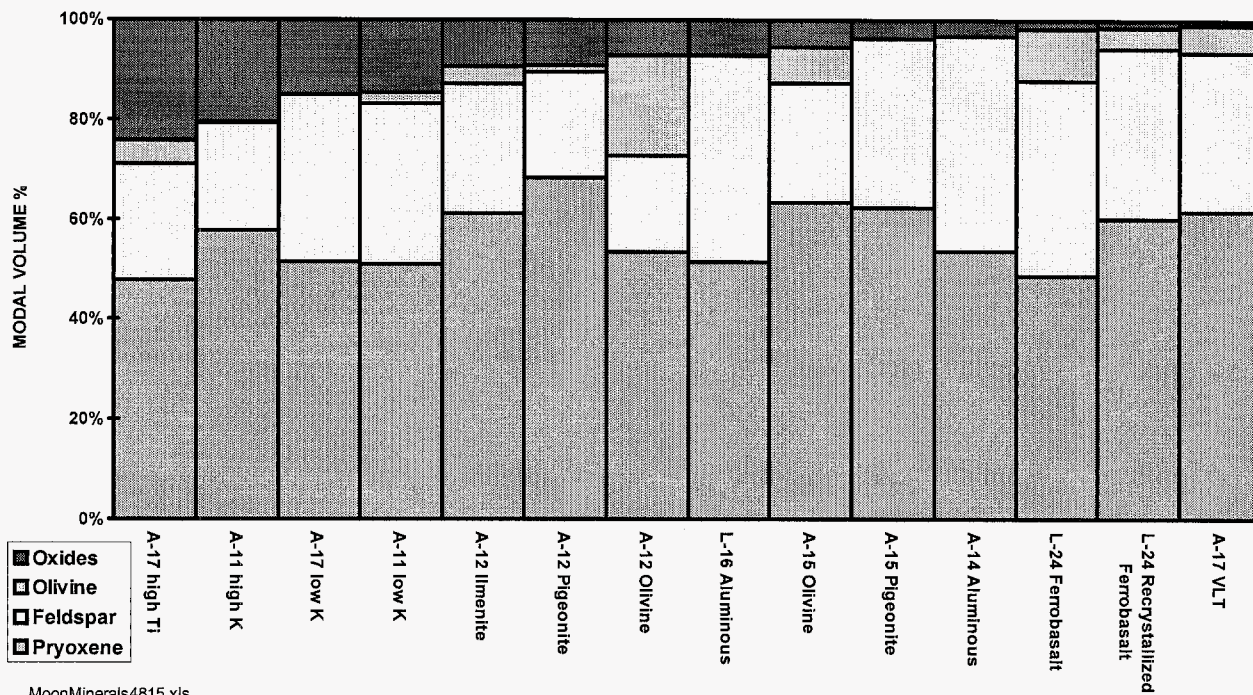


Figure 1. Lunar mare basalts from the Apollo and Luna sites.

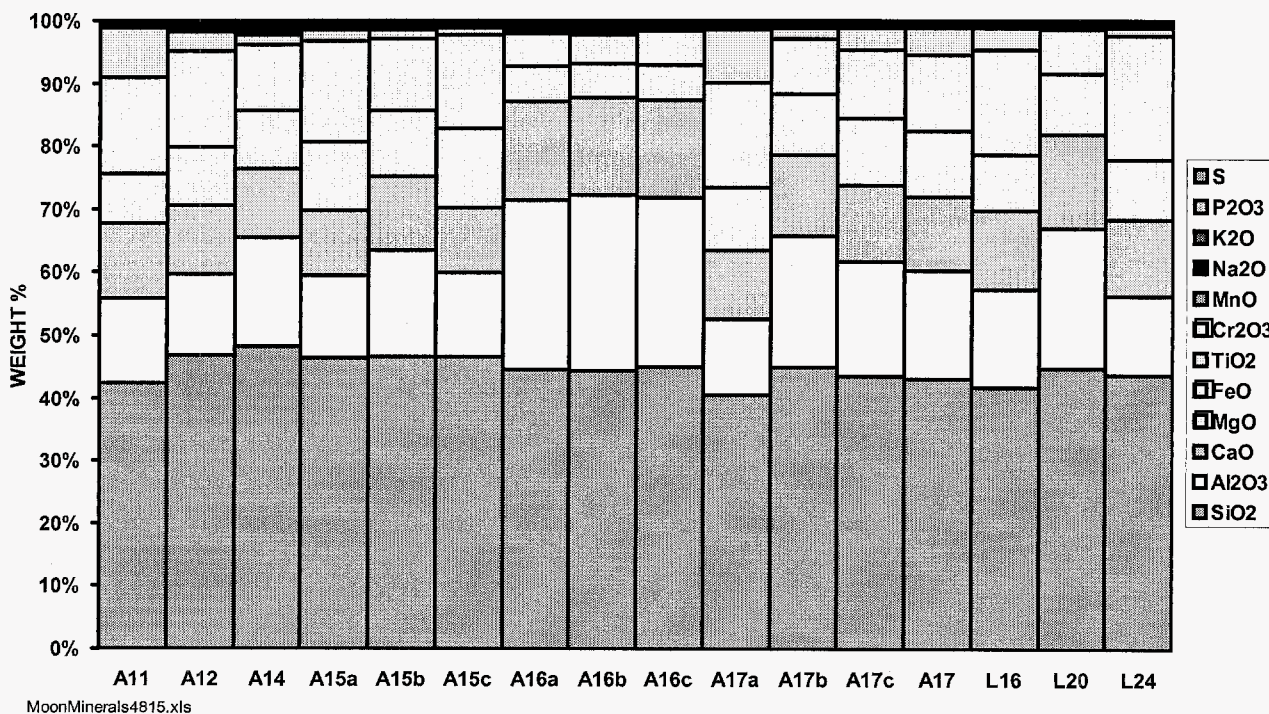


Figure 2. Lunar mare oxides from the Apollo (A) and Luna (L) sites.

The oxides are further displayed in Fig. 2. They are from Apollo and Luna sites. This chart indicates that silica is the

dominant oxide and is widely present in the lunar regolith. The other oxides that are of consequence (concentrations >1%) are Al₂O₃, CaO, MgO, FeO and TiO₂. The other oxides such as Cr₂O₃, MnO, Na₂O, K₂O, P₂O₃, and S are found in concentrations less than 1% and so are less interesting from an ISRU perspective.

Thus, the Moon is seen as very poor in mineral content compared to mineral abundances on Earth. In the following analysis, only the silicates and oxides are considered.

WHEEL-BASED SENSORS

The concept is shown in Fig. 3 where a number of sensors are exposed to the soil through the tread of the rover wheel. Our sensor selection is: (a) Impedance Spectrometer, (b) Ohmmeter, (c) Electrometer, (d) Magnetometer and (e) Temperature sensor.

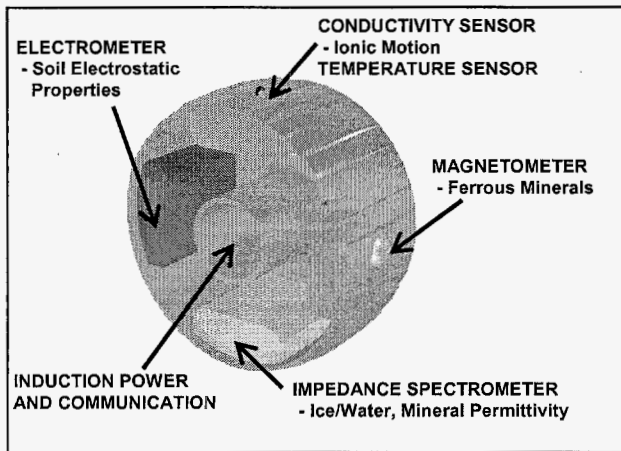


Figure 3. Proposed rover wheel with sensors for *in situ* soil measurements.

As indicated in the figure, we plan to use induction techniques to power the sensors and to communicate. Other techniques such as slip-rings and RF communications have been considered but do not appear to be as favorable as induction.

Our prospecting approach uses a two-tiered concept where the sensors in the wheel perform a quick scan of the regolith while the rover is in motion. The on-board computer then determines if the signals coming from the sensors are sufficiently different to warrant stopping the rover and performing a more detailed analysis using spectrometer instrumentation.

The contact time for the sensors can be estimated using the MER (Mars exploration Rover) as an example. The MER wheel, seen in Fig. 4, is 24-cm in diameter, has a 16-cm width, and a 0.5-cm rib depth. The maximum velocity is 3

cm/s which is about 0.06 km/hr. By way of contrast, the LRV (Lunar Roving Vehicle) on Apollo 15 had a wheel diameter of 82-cm and a cruise velocity of 6 km/hr. For the MER with a 1-cm penetration depth into the soil, the contact time is ~7 s. This is sufficient time to make measurements of the type contemplated here.

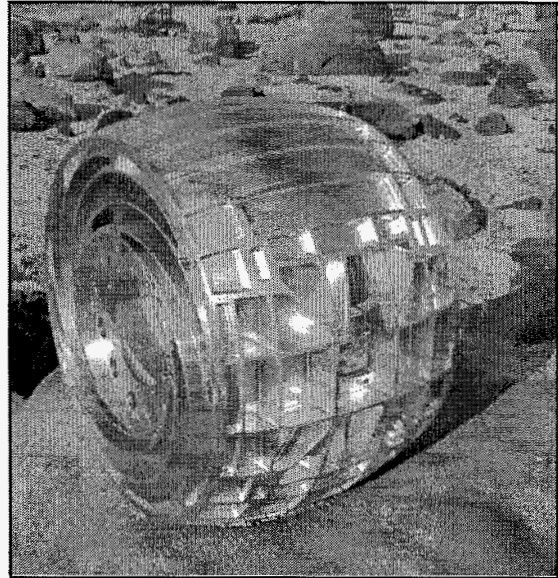


Figure 4. MER wheel showing the cavity for attaching the rover to the lander.

The sensor measurement sensitivity and range are listed Table 2. Also listed is the anticipated power which is about 1.4 W.

Table 2. Prospector Wheel Sensors

Sensor	Parameter Sensitivity	Parameter Range	Power W
Electrometer	1 pC	100 pC	0.10
Magnetometer	40 μGauss	± 2Gauss	0.35
Impedance Spectrometer	E' at 5% E'' at 5%	e' = 1 to 1000 e'' = 0.001 to 1	0.80
Conductivity Sensor	5%	10 ⁻⁸ to 10 ⁻² S/cm	0.10
Temperature Sensor	0.4 °C	-75 to +100 °C	0.01

IMPEDANCE SPECTROMETER

The impedance spectrometer builds on the existing effort to characterize soil conductivity. The impedance spectrometer we will implement includes the ability to measure both the real and imaginary permittivity of the soil and so provides

a measure of the soil conductivity (real permittivity) and the soil dielectric constant (imaginary permittivity).

The dielectric constant, ϵ , is expressed as the product of the permittivity of free space, ϵ_0 , times the relative permittivity, ϵ_r . The permittivity is further described as $\epsilon_r = \epsilon' - j\epsilon''$ where ϵ' is the real permittivity and ϵ'' is the imaginary permittivity [3].

1.1 Lunar Soils and Terrestrial Minerals

Measurements on Lunar soils are shown in Fig. 5. The data shown here were extracted from Table A9.16 from the LSB [2]. A total of 83 data points were analyzed. Six points were excluded from the data set because they did not have %TiO₂+%FeO values or the density was zero. All data with a density less than 2.1 g/cc were assumed to be lunar soils, as indicated in Fig. 9.5.3 LSB. The lunar soils were characterized by a number of investigator using different equipment, measurement frequencies (0.1, 1, 455, 9375 MHz), and environments (air, nitrogen, and vacuum).

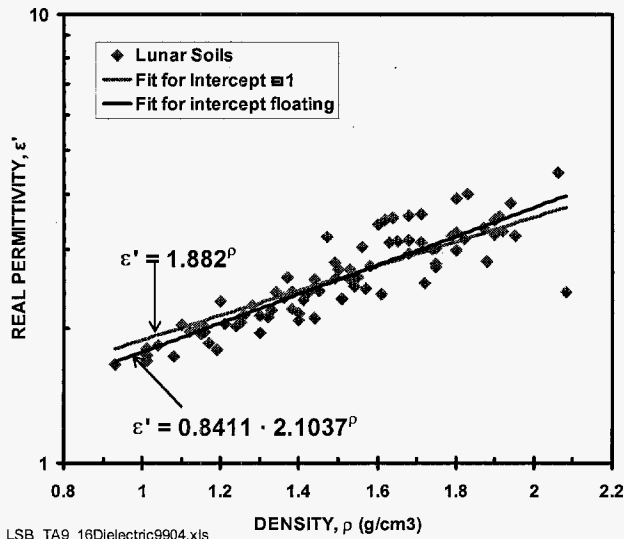
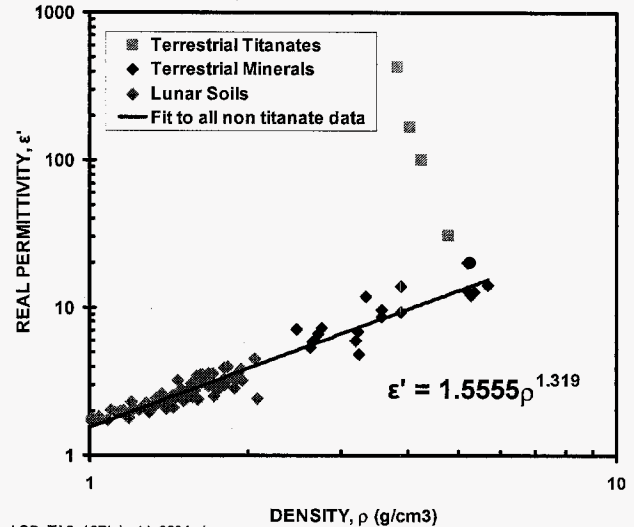


Figure 5. Real permittivity versus density for lunar soils

The real permittivity, ϵ' , shown in Fig. 5, indicates that it is proportional to the lunar soil density. This observation is constant with the conclusion presented in the LSB. Two equations were fitted to the data. One equation assumed that the intercept is unity when the density is zero. This assumption has a physical interpretation. That is, the relative permittivity is unity for a vacuum where the density is zero. The fitted number, 1.882, for the first equation is numerically close to the value of 1.871 shown in Fig. 9.53 LSB. The similarity of the two numbers gives confidence that the data were extracted faithfully from the LSB.

Another fit to the data is shown in Fig. 5. In fitting this equation, the intercept was extracted. One outlier point is visible at the highest density. It was included in the analysis but is a candidate for exclusion in future analyses.

Fig. 6 shows that the real permittivity, ϵ' , can be used to determine the density of minerals. The simple relationship shown in the figure holds for silicates and oxides with a few exceptions. As seen in Fig. 6, the titanates (and certain other minerals) have abnormally high permittivities.



LSB_TA9_16Dielectric9904.xls

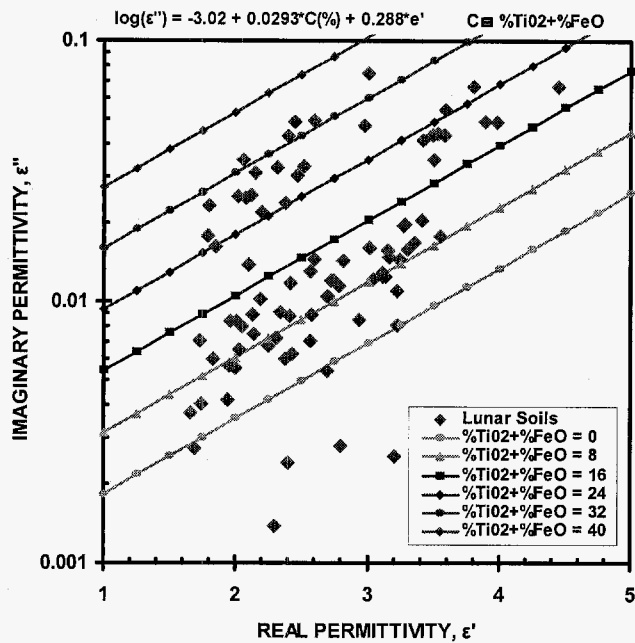
Figure 6. Real permittivity-density relationship for lunar soils and terrestrial minerals.

As seen in Fig. 6, the non titanate data are well fit by the power law function given in the figure. This graph shows that the real permittivity is a simple function for both soils that are porous and solid minerals where the space between the particle grains has been removed.

1.2 Imaginary Permittivity

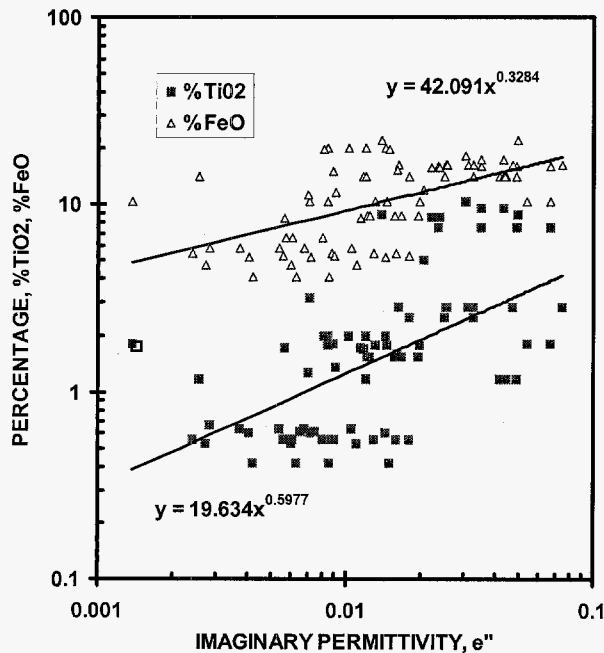
An important finding of our analysis is shown in Fig. 7. Here, the imaginary permittivity, ϵ'' , is plotted against ϵ' for various values of %TiO₂ + %FeO. This graph allows a direct determination of the amount of %TiO₂ + %FeO in the lunar soil. At the measured ϵ' , the amount of %TiO₂ + %FeO is determined from ϵ'' . Four outlier data points appear at low values for %TiO₂ + %FeO. Reasons for excluding them from future analyses are being pursued.

Further justification for the interpretation of the data seen in Fig. 7 is shown in Fig. 8. This plot shows the dependence of %TiO₂ and %FeO on ϵ'' . This is further evidence that ϵ'' can be used to determine the %TiO₂ + %FeO.



LSB_TA9_16Dielectric9904.xls

Figure 7. The percentage of TiO₂ and FeO can be determined by measuring the real and imaginary part of the permittivity. The measured data are for lunar soils obtained from the Apollo missions.



LSB_TA9_16Dielectric9904.xls

Figure 8. Dependence of the percent TiO₂ and FeO on the imaginary permittivity.

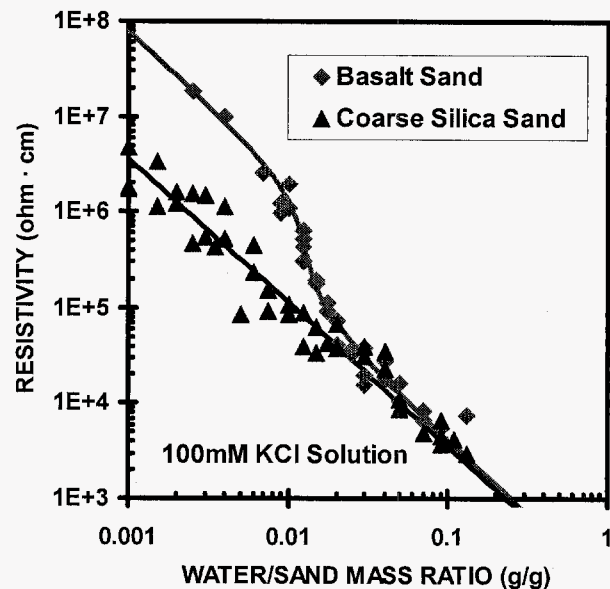
ELECTRICAL RESISTIVITY

The resistivity of lunar soils is quite high being between 10^{12} to 10^{16} ohm-cm at 23 °C [2]. The resistivity is temperature dependent and there is a significant photoconductivity effect. The lunar soils show at 10^6 decrease in resistivity in the UV [2].

In this section our instrument capability is illustrated using silica sand and basalt with various amounts of moisture. These measurements are focused at characterizing the moisture estimated to be found in Martian soils. This requirement has taught us the techniques for making high resistivity soil measurements.

1.3 Moisture detection

Results for coarse silica sand and basalt sand are shown in Fig. 9. This data shows that measurements were acquired over the range from 0.1% to 15% moisture by weight using the resistivity sensor found on E-Tongue 3 [4].

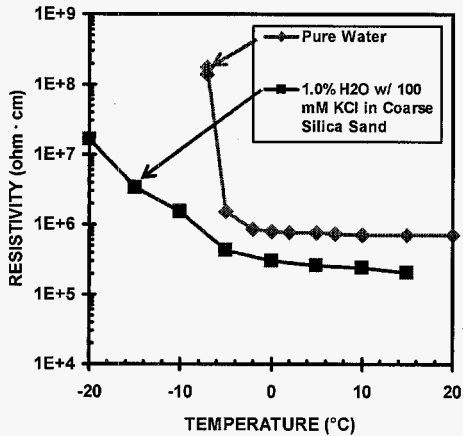


UNR2004Matrix40803Final.xls

Figure 9. Resistivity of two types of moist sand at room temperature.

1.4 Permafrost

The same procedure used to prepare the samples for the room temperature measurements shown in Fig. 9 were used in acquiring the temperature data shown in Fig. 10 for the coarse silica sand sample. In addition to the sand measurements, water measurements were also acquired.



UNR2004Matrix40803Final.xls

Figure 10. Temperature dependence of coarse silica sand with temperature.

These results show an increase in the resistivity of the mixture as the temperature is decreased below 0 °C. The resistivity behavior of the water and sand with temperature are similar to those noted by Scott [5]. They too observed that large increase in resistivity with decreasing temperature. This data also shows our capability to make measurements at low temperatures and at high resistivity values. Currently, the equipment is limited to resistivities less than 10^9 ohm-cm. This limit is due the choice of scaling resistors. We plan to expand our measurement range well into the Gohm-cm range.

ELECTROMETER

1.5 Electrometer

The electrometer shown in Fig. 11 was developed for the MECA project [6]. Results of rocking experiments are shown in Fig. 12-15. They indicated that soils have different signatures and can be used to determine when the rover wheel is traversing a new soil.

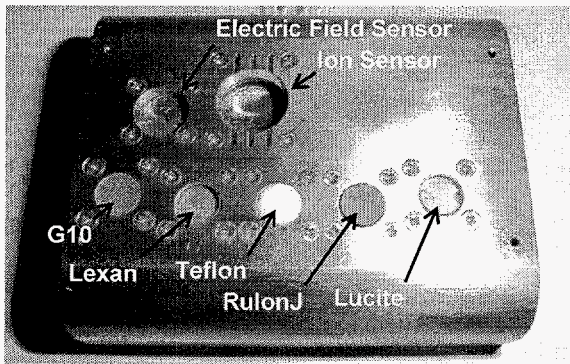


Fig. 11. Electrometer developed at for MECA '01.

1.6 Ottawa Sand

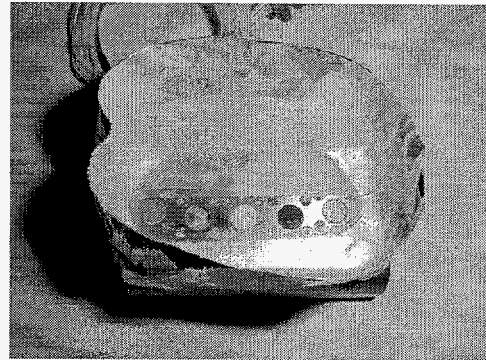


Fig. 12a. Ottawa sand: No sand dust on insulators.

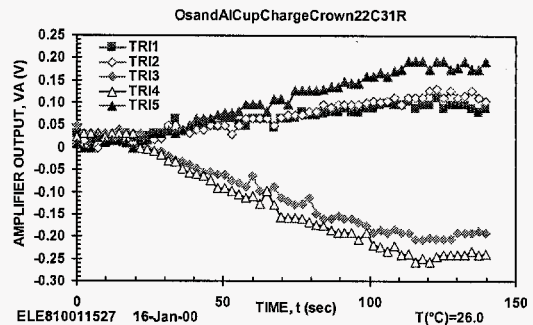


Fig. 12b. Ottawa sand. Results governed by contact triboelectrification

1.7 Basalt

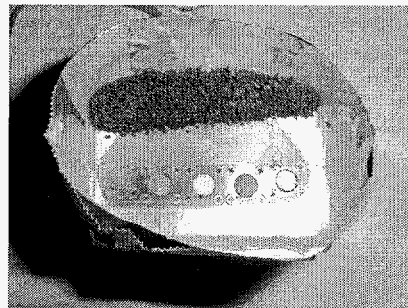


Fig. 13a. Basalt: No basalt dust on insulators

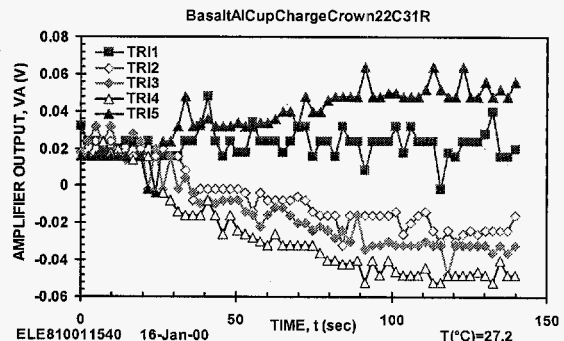


Fig. 13b. Basalt response.

1.8 Titanium Dioxide

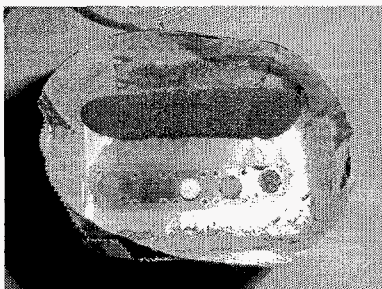


Fig. 14a. Titanium dioxide: Dust coated TRI2 and TRI5.

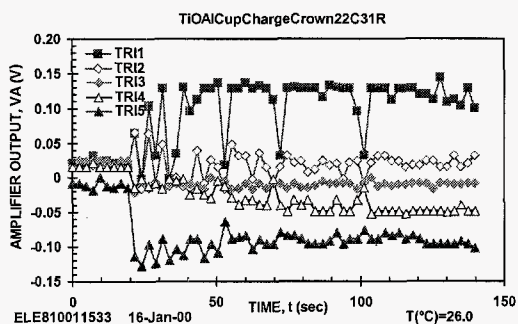


Fig. 14b. Titanium dioxide response. Dust coats insulators

1.9 Hematite

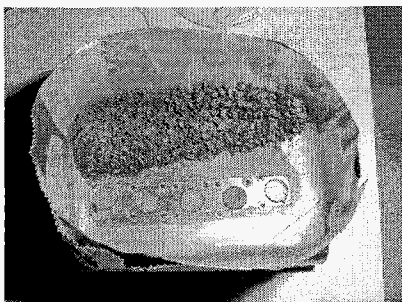


Fig. 15a. Hematite: Dust covers insulators. This is especially apparent for TRI3 (Teflon).

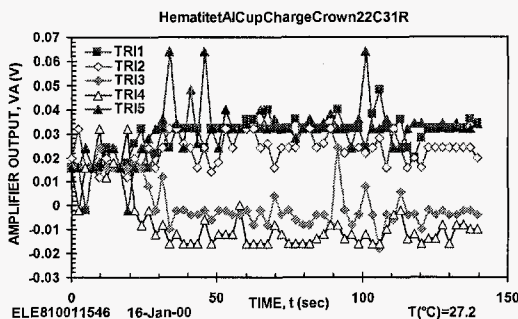


Fig. 15b. Hematite. Dust coats insulators

By taking data from Figs. 12-15 after 100 s rubbing exposure, a histogram was constructed as seen in Fig. 16

that shows that the response for each mineral is different and unique. This figure provides the basis for signature analysis of the electrometer data.

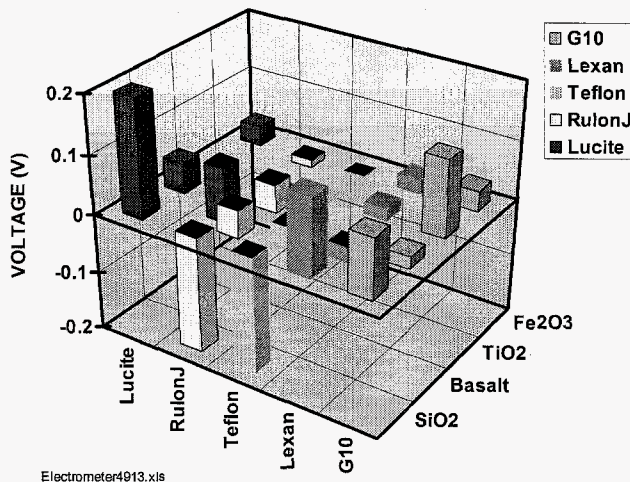


Figure 16. Response surface for the electrometer exposed to four minerals.

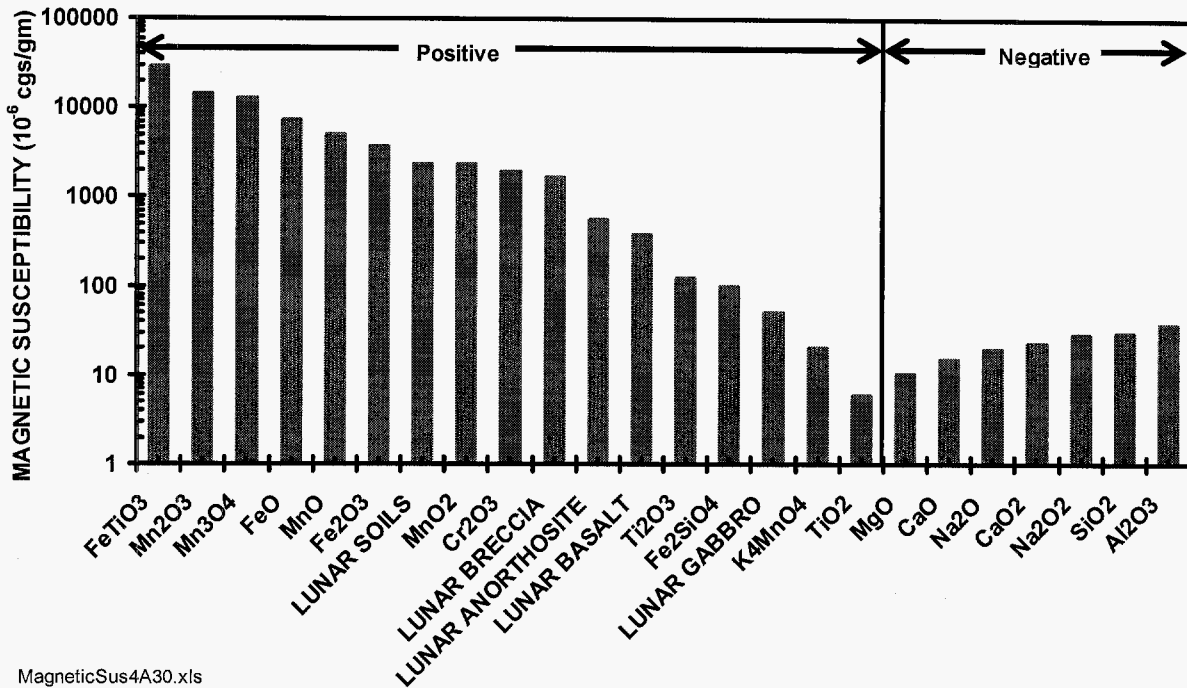
The electrometer has been fabricated into a wheel and tested by Calle and co-workers [7] at the Kennedy Space Center. They have performed measurements using the JSC Mars soil simulant [8] and the results indicate that different insulators have different responses to the simulant indicating the viability of the measurement.

MAGNETOMETER

To further characterize the lunar materials, the magnetic properties of the lunar regolith will be measured using a magnetometer. The magnetometer will have a sensitivity of The magnetic susceptibility of a mineral is a measure of the induced magnetism in that material.

The magnetic properties of lunar soils and minerals returned from the Apollo missions was characterized by a number of investigators [9]. The magnetic susceptibility of these materials is shown in Fig. 17 long with values for terrestrial minerals. The value for the susceptibility can have either a positive or negative value. The positive susceptibility indicates minerals with high retained magnetism; whereas negative susceptibility indicate minerals with little or retained magnetism.

The lunar minerals are plotted in Fig. 17 along with minerals likely to be found on lunar surface. As seen in the figure, the lunar minerals have a significant magnetic susceptibility. Another observation is that the lunar soils have the largest susceptibility when compared with other lunar minerals.



MagneticSus4A30.xls

Figure 17. Magnetic susceptibility of lunar and terrestrial minerals.

CONCLUSION

Lunar minerals are mostly silicates and oxides. This lack of diversity of minerals on the moon can be exploited in a number of ways. First, the real permittivity of the lunar soils is proportional to density. This greatly simplifies density measurements. Second, the imaginary part of the permittivity can be used to identify the presence of important minerals such as TiO₂ and FeO. Third, because the moon is very dry, electrostatic measurements can be used to identify difference in mineral types. Forth, The lunar soils have a reasonably high magnetic susceptibility which indicates the presence of important minerals. Finally, the measurements proposed here can be incorporated into the wheel of a rover and used to prospect for minerals important for ISRU.

ACKNOWLEDGMENTS

The work described in this paper was performed by the Jet Propulsion Laboratory, California Institute of Technology, under a contract with the National Aeronautics and Space Administration. The overall effort is supported by an ASTID02 entitled "An instrument for detecting water, brines and signatures of microbial activity on Mars and Europa". The authors are indebted to Walter Russel, Soil Physics Department, USDA-ARS George E. Brown, Jr. Salinity Laboratory for extracting the data from the LSB. File: AeroProspector4A22.doc.

REFERENCES

- [1] W. Feldman, et al., "Fluxes of Fast and Epithermal Neutrons from Lunar Prospector: Evidence for Water Ice at the Lunar Poles", *Science*, Vol. 281, p. 1496, 1998.
- [2] Heiken, G., D. Vaniman, and B. M. French, "Lunar Sourcebook, Cambridge University Press (New York, 1991).
- [3] J. C. Anderson, *Dielectrics*, Reinhold Publishing Corp. (New York, 1964)
- [4] M. Buehler, G. Kuhlman, D. Keymeulen, N. Myung, and S. Kounaves, "Planar REDOX and Conductivity Sensors for ISS Water Quality Measurements", *Aerospace Conference, 2003. Proceedings. 2003 IEEE, Volume: 2, March 8-15, 2003*, pages 2_527 – 2_533
- [5] Scott, W.J., Sellmann, P.V, and Hunter, J.A, 1990, Geophysics in the study of permafrost. In *Geotechnical and Environmental Geophysics*, Vol 1. Ed. S.H.Ward, SEG
- [6] M. Buehler, L-J. Cheng, O. Orient, Michael Thelen, R. Gompf, J. Bayliss, and J. Rauwerdink, "MECA Electrometer: Initial Calibration Experiments" *Electrostatics 1999, Proceedings of the 10th International Conference*, Institute of Physics Conference Series No. 163

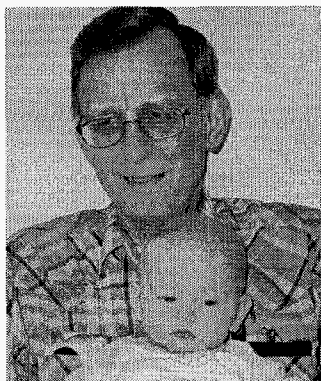
pp. 189-196 (Institute of Physics Publishing, Bristol, UK, 1999)

[7] C. I. Calle, J.G. Mantovani, C.R. Buhler, E.E. Groop, M.G. Buehler, A.W. Nowicki, "Embedded Electrostatic Sensors for Mars Exploration Missions", *Journal of Electrostatics* 61 (2004) 245-257

[8] C. C. Allen, et al., "Martian Regolith Simulant JSC MARS-1", *Luna rand Planetary Science*, XXIX 1998.

[9] R. S. Carmichael, *Practical Handbook of Physical Properties of Rocks and Minerals*, CRC Press (Boca Raton, Florida, 1990)

BIOGRAPHIES



Martin G. Buehler received the BSEE and MSEE from Duke University in 1961 and 1963, respectively and the Ph.D. in EE from Stanford University in 1966 specializing in Solid State Electronics under G. L. Pearson and W. Shockley. He worked at Texas Instruments for six years, at National Bureau of

Standards (now NIST) for eight years, and since 1981 has been at the Jet Propulsion Laboratory where he is a senior research scientist. At JPL he developed p-FET radiation monitors for CRRES, Clementine, TELSTAR and STRV, E-nose which flew on STS-95 with John Glenn, an electrometer for the Mars '01 robot arm and E-Tongue for ISS water quality. Currently, he serves on the staff of the New Millennium Program as a technical analyst. Martin is a life member of the IEEE, and a member of Tau Beta Pi, and Sigma Nu. He holds 13 patents and has published over one hundred papers.



Robert C. Anderson received the Bachelor Science Degree in geology in 1979 and in 1979 received the Master of Science from Old Dominion University in geology with emphasis on structural geology and mapping tectonic features surrounding the Tharsis region of Mars. In 1995, he received a Doctor of Philosophy from the University of Pittsburgh in geology with

emphasis on visible and near-infrared remote sensing. His Ph.D. research was centered on mapping young Quaternary

surfaces, desert pavements and varnish, and soils around the Whipple Mountains of southwestern Arizona to better understand the past climatic history of the region. Bob joined JPL in 1996 where he has contributed to the Mars Pathfinder Project as the science coordinator of the Mineralogy and Geochemistry Science Operations Group. Next he was he was Deputy Director of Mars Education and then Mission Planner for the Mars 2001 lander. His current science research is centered on unraveling the geologic history of Mars with emphasis on understanding the tectonic, structural, paleohydrologic evolution of the Tharsis region. He is a Senior member of the Technical Staff at JPL and is currently employed as the Investigation Scientist for the Rock Abrasion Tool (RAT), Soil properties, and science support for Mission Operations on the Mars 03 mission. He is presently Adjunct Research Faculty at the University of Pittsburgh Department of Geology and Planetary Science as well as Adjunct Faculty at Pasadena City College where he is presently teaching a class on Planetary Geology.



Marcel G. Schaap received a BA in Chemistry (1984) and a MS (1990) and PhD (1996) in Soil Chemistry and Soil Physics from the University of Amsterdam, the Netherlands, specializing in the measurement and modeling of soil water contents and soil electric conduction. In

1996 he joined UC Riverside and, through a collaborative agreement, the George E. Brown, Jr. Salinity Laboratory, where he developed artificial neural network based software for the estimation of soil hydraulic properties. His current interests are the measurement and modeling of soil dielectric properties, development of high-precision automated soil hydraulic measurements, and the modeling of micro-scale fluid flow and interfacial phenomena with Lattice Boltzmann Models. He has published over 30 peer-reviewed papers on soil and environmental chemistry and physics.